



# Runx2 overexpression promotes bone repair of osteonecrosis of the femoral head (ONFH)

Hai-Jia Xu<sup>1</sup> · Xiang-Zhong Liu<sup>1</sup> · Lu Yang<sup>2</sup> · Yu Ning<sup>3</sup> · Liang-Liang Xu<sup>4</sup> · Da-Ming Sun<sup>4</sup> · Wen Liao<sup>1</sup> · Yi Yang<sup>4</sup> · Zhang-Hua Li<sup>1</sup>

Received: 14 November 2022 / Accepted: 28 March 2023 / Published online: 7 April 2023  
© The Author(s) 2023

## Abstract

**Background** Runt-related transcription factor-2 (Runx2) has been considered an inducer to improve bone repair ability of mesenchymal stem cells (MSCs).

**Methods and results** Twenty-four rabbits were used to establish Osteonecrosis of the femoral head (ONFH) and randomly divided into four groups: Adenovirus Runx2 (Ad-Runx2) group, Runx2-siRNA group, MSCs group and Model group. At 1 week after model establishment, the Ad-Runx2 group was treated with  $5 \times 10^7$  MSCs transfected through Ad-Runx2, the Runx2-siRNA group was treated with  $5 \times 10^7$  MSCs transfected through Runx2-siRNA, the MSCs group was injected with  $5 \times 10^7$  untreated MSCs, and the Model group was treated with saline. The injection was administered at 1 week and 3 weeks after model establishment. The expression of bone morphogenetic protein 2 (BMP-2), Runx2 and Osterix from the femoral head was detected at 3 and 6 weeks after MSCs being injected, and Masson Trichrome Staining, Gross Morphology, X-ray and CT images observation were used to evaluate the repair effect of ONFH. The data revealed that the expression of BMP-2, Runx2 and Osterix in the Runx2-siRNA group was reduced at 3 weeks compared with the MSCs group, and then the expression further reduced at 6 weeks, but was still higher than the Model group besides Osterix; The expression of these three genes in the Ad-Runx2 group was higher than in the MSCs group. Masson Trichrome Staining, Gross Morphology and X-ray and CT images observation revealed that necrotic femoral head of the MSCs group was more regular and smooth than the Runx2-siRNA group, which has a collapsed and irregular femoral head. In the Ad-Runx2 group, necrotic femoral head was basically completely repaired and covered by rich cartilage and bone tissue.

**Conclusions** Overexpression of Runx2 can improve osteoblastic phenotype maintenance of MSCs and promote necrotic bone repair of ONFH.

**Keywords** Osteonecrosis of the femoral head · Mesenchymal stem cells · Runx2 · Bone repair

---

Hai-Jia Xu, Xiang-Zhong Liu and Lu Yang have contributed equally to this work.

✉ Zhang-Hua Li  
lizhanghua\_123@163.com

- <sup>1</sup> Department of Orthopedics, Wuhan Third Hospital, Tongren Hospital of Wuhan University, Wuhan 430060, China
- <sup>2</sup> Department of Anesthesiology, Wuhan Third Hospital, Tongren Hospital of Wuhan University, Wuhan 430060, China
- <sup>3</sup> Department of Orthopedics, XiangYang Hospital of Traditional Chinese Medicine, Hubei University of Chinese Medicine, Xiangyang 441000, China
- <sup>4</sup> Wuhan Sports University, Wuhan 430079, China

## Introduction

ONFH is a common bone disease featured by interruption of angiogenesis, bone cell and bone marrow death, bone collapse, with about 75% of patients aged 30 to 60 years. Its etiology is very complex, including but not limited to trauma, overdose of glucocorticoids administration and excessive drinking [1–4]. Early diagnosis and treatment can prevent the progression of joint destruction, reduce the implementation of traumatic surgery, and improve the probability of hip preservation, such as some lncRNA, ultrasound molecular imaging, core decompression, osteotomy and physical therapy, etc. However, these methods are usually not very satisfactory, approximately 40% of patients progressing to total hip arthroplasty [5–8]. MSCs are considered to be an

ideal material for bone regeneration and vascular regeneration because of its differentiation potency [9, 10].

In recent years, stem cells transplantation has been one of the most common methods for the treatment of ischemic diseases [11]. Mastrolia and his colleagues confirmed bone formation through transplanting autologous MSCs to treat ONFH [12]. In our previous experiments, a large number of high-purity allogeneic MSCs have been confirmed to migrate, survive and proliferate in necrotic bone, and will not cause acute or chronic immune rejection and manifestations of graft-versus-host disease [13]. Further animal experiments confirmed that allogeneic MSCs can improve osteonecrosis blood supply and promote bone regeneration [14]. However, Simple MSCs transplantation have some shortcomings, such as a large number of cells are needed, multiple transplants are needed, long time to repair is needed and unstable differentiation ability without induction. Some methods have been used to induce MSCs differentiate into osteoblasts, These methods mainly include drugs, physical stimulation, exosomes, gene transfection and platelet lysate and so on [15–22].

As the core binding factor  $\alpha 1$  (Cbfa1), Runx2 belongs to the RUNT transcription factor family which is expressed in MSCs and osteochondral progenitor cells, performing as a “master” regulator of osteogenesis [23–25]. But there is not direct evidence that MSCs overexpressing Runx2 can repair ONFH. In this paper, MSCs were injected into ONFH rabbit model after being transfected with Adenovirus Runx2, and histological, radiologic and molecular analyses were used to detect the repair effect.

## Materials and methods

### MSCs isolation and identification

MSCs were isolated according to the previous method [26]. In brief, bone marrow of the four limbs was obtained by flushing with 26-gauge syringe needle containing phosphate-buffered saline (PBS) under sterile conditions. The contents were washed and centrifuged at 1500 rpm for 5 min. And then MSCs was resuspended with mesenchymal stem cell medium (MSCM, Sciencell, USA) and maintained in a 37 °C incubator with 5% CO<sub>2</sub>. MSCs were observed under a fluorescence inverted microscope (Leica, Germany) and passaged when they reached 80–90% confluence.

For phenotypic characterization,  $5 \times 10^5$  MSCs were trypsinized and washed twice with PBS, and were incubated with fluorescein isothiocyanate (FITC)-conjugated anti-CD29 (ab255354), anti-CD44 (ab189524) and anti-CD45 (ab40763) (all from Abcam, USA) at a dilution rate of 1: 500 for 30 min at 4 °C. Then, MSCs were washed

twice with PBS again and analyzed by CytoFLEX S Flow cytometry (Beckman, USA).

For adipogenic and osteogenic differentiation,  $2 \times 10^4$  MSCs were seeded in a 6-well plate and maintained with osteogenic differentiation medium and adipogenic differentiation medium (Cyagen, USA) for 3 weeks. Mineralized nodule and lipid droplets were detected by alizarin red and Oil red O staining kit (Cyagen, USA), and observed under a fluorescence inverted microscope.

### Ad-Runx2 and Runx2-siRNA transfection

Third passage MSCs were transfected with Ad-Runx2 (was synthesized in Shanghai Jikai Biotech Co., Ltd) and Runx2-siRNA (was synthesized in Guangzhou Ribobio Biotech Co., Ltd) according to manufacturer's instructions and previous research [26]. Briefly, Ad-Runx2 with Green Fluorescence Protein (GFP) fluorescence was mixed with Dulbecco's Modified Eagle's Medium (DMEM, meilunbio, China) and was added to MSCs followed by incubation for 6 h. Then, MSCM was added followed by incubation for 72 h. Runx2-siRNA with CY3 fluorescence and lipofectamine 2000 (Thermo fisher, USA) were diluted by DMEM for 5 min, and they are mixed followed by incubation for 20 min. Then, the mixture was added to MSCs followed by incubation for 72 h.

### Western blot analysis

Western blot analysis was used to detected the protein level of BMP-2 (ab6285), Runx2 (ab114133), Osterix (ab94744) (all from Abcam, USA) and glyceraldehyde-3-phosphate dehydrogenase (GAPDH, ab9485). Total protein was extracted and its concentration was measured by BCA assay kit (Servicebio, China) followed by mixing with 5×loading buffer at 95 °C for 5 min. Total protein of each group was separated by 10% SDS-PAGE at 60 V for 30 min and 100 V for 1 h, and transferred to a PVDF membrane (Millipore, USA) at 200 mA for 1 h. The PVDF memberane was blocked with 5% skim milk for 1 h and incubated with primary antibodies against BMP-2 (1:2000), Runx2 (1:1000), Osterix (1:2000) and GAPDH (1:5000) at 4 °C overnight. The memberane was incubated with secondary antibodies (1:7000) at room temperature for 1 h after being washed three times with washing buffer. Then, The member was incubated with enhanced chemiluminescence (Biorad, USA) and exposed by the gel imaging system (Biorad, USA). GAPDH was employed as the internal reference and each experiment was performed in triplicate. The Image J software was used for grayscale determination.

## Quantitative real-time PCR (qPCR) analysis

Total RNA was extracted by the Trizol RNA Extracting Solution (TOYOBO, Japan) and reverse-transcribed into cDNA by a cDNA synthesis kit (TOYOBO, Japan). The relative mRNA expression levels of BMP-2, Runx2, Osterix and GAPDH were detected through SYBR Green Realtime PCR Master mix (TOYOBO, Japan). The primer sequences were synthesised at SANGON Biotech Co, Ltd (Shanghai, China). The primer sequences are shown in Table 1.

qPCR was performed by the Bio-Rad CFX Manager system (Bio-Rad, USA), including 10  $\mu$ L of 2  $\times$  ultraSYBR mixture, 1  $\mu$ L of forward primer and reverse primer, 1  $\mu$ L of cDNA and ddH<sub>2</sub>O 7  $\mu$ L. Reaction conditions were as follows: pre-denaturation at 95 °C for 3 min, 40 cycles of denaturation at 95 °C for 10 s, annealing at 60 °C for 10 s and extending at 72 °C for 10 s. The relative expression of mRNAs was calculated by the  $2^{-\Delta\Delta Ct}$ . GAPDH was employed as the internal reference and each experiment was performed in triplicate.

## Model establishment and MSCs transplantation

Twenty-four rabbits (body weight  $2.5 \pm 0.5$  kg) provided by the Animal Facility of the Wuhan wan qian jia xing Biotech Co., Ltd (Licence No. SCXK Hubei 2019-0011), without a specific requirement for sex. They were raised in a single cage with a normal diet. These rabbits were randomly divided into four groups: Ad-Runx2 group, Runx2-siRNA group, MSCs group and Model group.

The rabbit model of femoral head necrosis was established according to the previous method [18]. Briefly, the articular surface of femoral head was completely exposed under sterile conditions and treated with liquid nitrogen for 3–5 min until the color of the articular cartilage turned pale. Femoral head was immediately re-warmed in saline at 37 °C for 3 min. The wound was closed and sutured. Then 800 KU of penicillin was injected intramuscularly for 5 consecutive days.

At 1 week after model establishment,  $5 \times 10^7$  MSCs transfected with Ad-Runx2 (about 0.4 mL of cell solution),  $5 \times 10^7$  MSCs transfected with Runx2-siRNA (about 0.4 mL of cell solution),  $5 \times 10^7$  MSCs (about 0.4 mL of cell solution) and 0.4 mL saline were intravenously injected into Ad-Runx2 group, Runx2-siRNA group, MSCs group and

Model group respectively. The injection was administered at the 1 week and 3 weeks after model establishment. The femoral head was detected at the 3 and 6 weeks after MSCs being injected.

## X-ray and Micro CT Imaging

X-ray and Micro CT were taken to detect the necrotic femoral head. The scanning parameters of Micro CT were 5 mm thickness, 120 kV tube voltage and 60 mA tube current. Imaging analysis was used for qualitative observation of lesion location, size, conformation, marginal and internal structure, and secondary changes.

## Statistical analysis

Data were expressed as mean  $\pm$  standard deviation (SD) and analyzed with SPSS 23.0 statistical software (SPSS, Chicago, IL, USA). Comparisons among groups was conducted with one-way ANOVA.  $P < 0.05$  was considered a statistically significant difference.

## Results

### Identification of MSCs

MSCs were exhibited whirl-like growth under low-power microscope, and displayed long spindle-shaped and fibroblast-like under high-power microscope (Fig. 1A). After adipogenesis and osteogenesis induction for 3 weeks, Oil red O staining showed lipid droplets, and alizarin red staining showed mineralized nodule (Fig. 1B, C). Flow cytometry showed that MSCs were positive for CD29 and CD44, but negative for CD45 (Fig. 1D).

### Transfection efficiency test of Ad-Runx2 and Runx2-siRNA

Green and red fluorescence from GFP and CY3 were observed evidently under a fluorescence inverted microscope (Fig. 2A and E). qPCR and Western blot were used to detect the mRNA and protein levels of Runx2 respectively. These results demonstrated that compared with the blank group, the Ad-Runx2 transfection group exhibited a significantly

**Table 1** Primer sequences

Forward Primer (5'-3')	Reverse Primer (5'-3')
BMP-2 TGTGGACTTCAGTGATGTG	TGGAGTTCAGGTGGTCAG
Runx2 GACTGTGGTTACCGTCATGGC	ACTTGGTTTTTCATA ACAGCGGA
Osterix TCCCTGGATATGACTCATCCCT	CCAAGGAGTAGGTGTGTGTC
GAPDH CTGGGCTACACTGAGCACC	AAGTGGTCGTTGAGGGCAATG

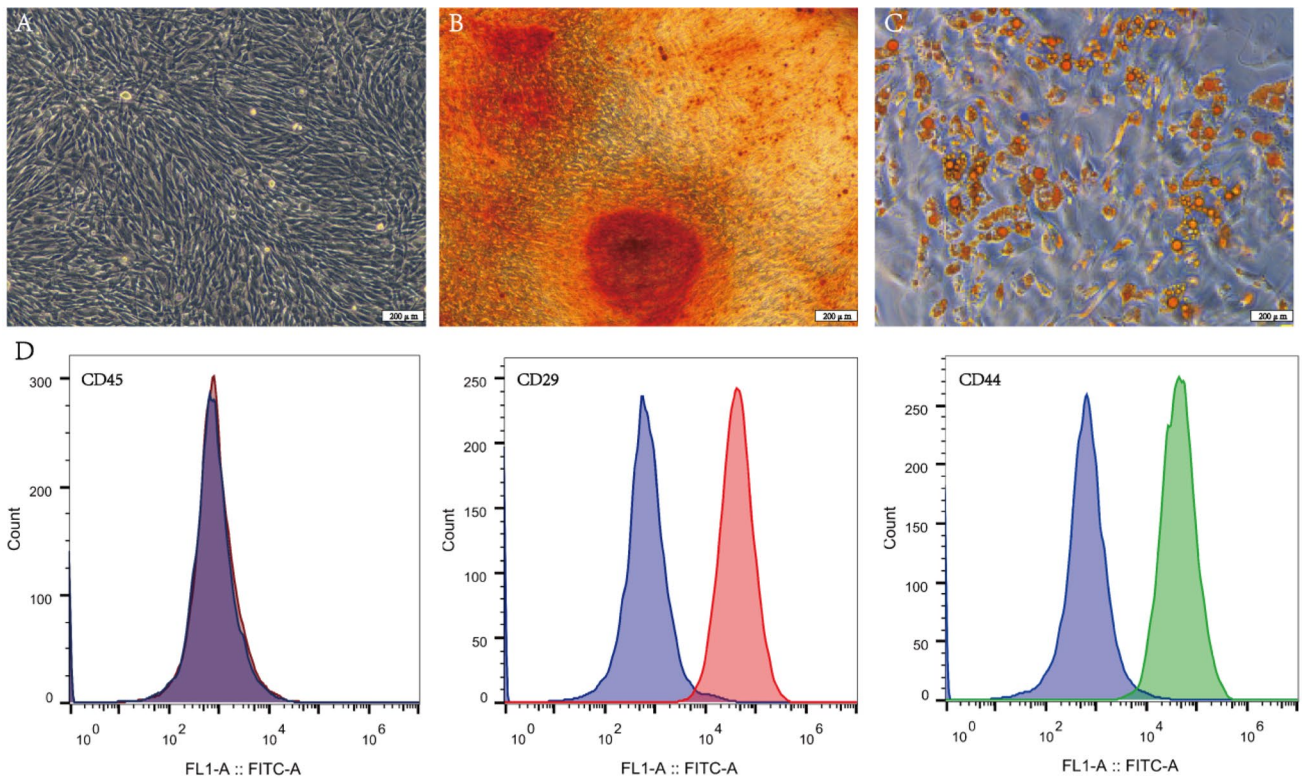


**Fig. 1** Cultivation and identification of MSCs. ( **A** The morphology of P3 MSCs was observed by microscopy. **B** The mineralized nodules of MSCs were screened by alizarin red staining. **C** The lipid droplets

of MSCs were screened by Oil red O staining. **D** Flow cytometry was used to identify cell surface markers (CD29, CD44, CD45)

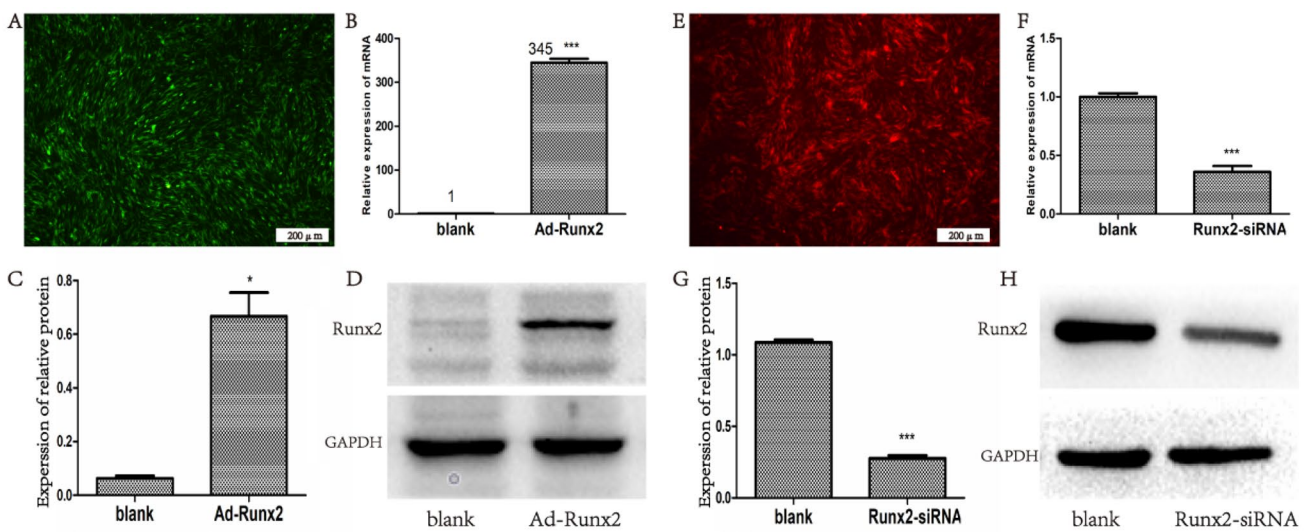


**Fig. 2** Ad-Runx2 and Runx2-siRNA transfection efficiency test. **A** and **E** The GFP and CY3 fluorescent distribution of MSCs was observed. **B** and **F** The mRNA level of Runx2 determined by qPCR.

**C**, **D**, **G** and **H** The protein level of Runx2 measured by Western blot analysis. \* $P < 0.05$  and \*\*\* $P < 0.001$  compared with the blank group respectively

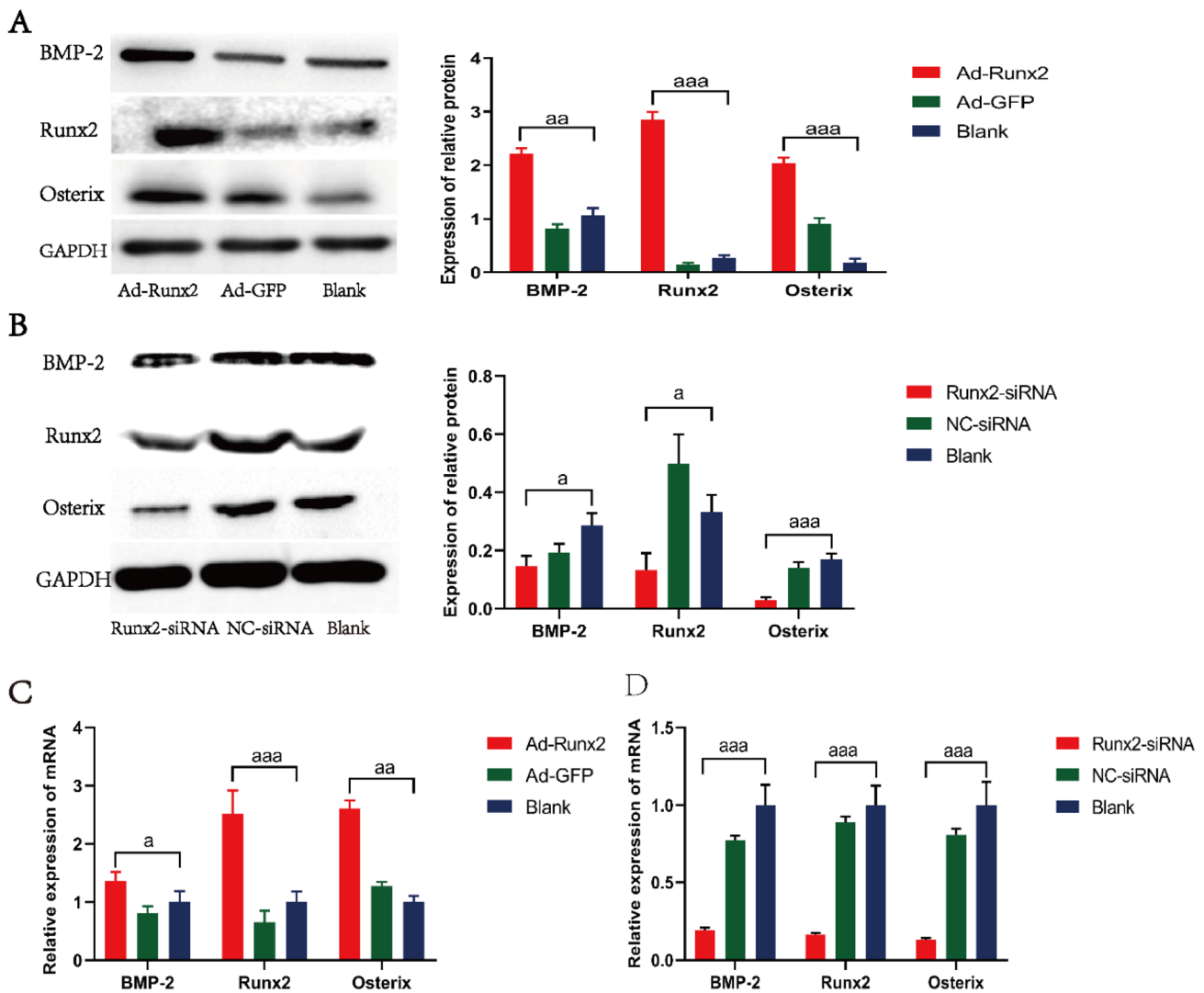


**Fig. 3** Runx2 overexpression induces osteogenic differentiation of MSCs. **A** and **B** The BMP-2, Runx2 and Osterix determined by Western blot; **C** and **D** The BMP-2, Runx2 and Osterix determined by qPCR; <sup>a</sup> $P < 0.05$ , <sup>aa</sup> $P < 0.01$  and <sup>aaa</sup> $P < 0.001$  compared with the blank group;

increased expression of Runx2 ( $P < 0.001$ ) (Fig. 2B, D), the Runx2-siRNA transfection group exhibited a completely inhibited effect ( $P < 0.001$ ) (Fig. 2F, G, H).

### Runx2 affected the osteogenic differentiation of MSCs

Western blot and qPCR were used to detect the expression of osteoblastic phenotype after MSCs being transfected by Ad-Runx2 and Runx2-siRNA. The results of Western blot and qPCR demonstrated that compared with the blank group, the Ad-Runx2 transfection group exhibited a significantly increased expression of BMP-2, Runx2 and Osterix ( $P < 0.05$ ) (Fig. 3A C), the Runx2-siRNA transfection group exhibited a significantly decreased expression of BMP-2, Runx2 and Osterix ( $P < 0.05$ ) (Fig. 3B and

D). These results showed that Runx2 overexpression can induce the osteogenic differentiation of MSCs.

### Overexpression of Runx2 promotes the expression of osteoblastic phenotype

qPCR and Western blot were used to detect the expression of osteoblastic phenotype from the femoral head at 3 and 6 weeks after MSCs being injected into ANFH models. The results of Western blot at 3 weeks revealed that compared with the Model group, the expression of BMP-2, Runx2 and Osterix were up-regulated significantly in the Ad-Runx2, Runx2-siRNA and MSCs groups ( $P < 0.05$ ). Compared with the MSCs group, the Ad-Runx2 group presented a significantly augmented BMP-2, Runx2 and Osterix ( $P < 0.05$ ); However, the Runx2-siRNA group showed a significant

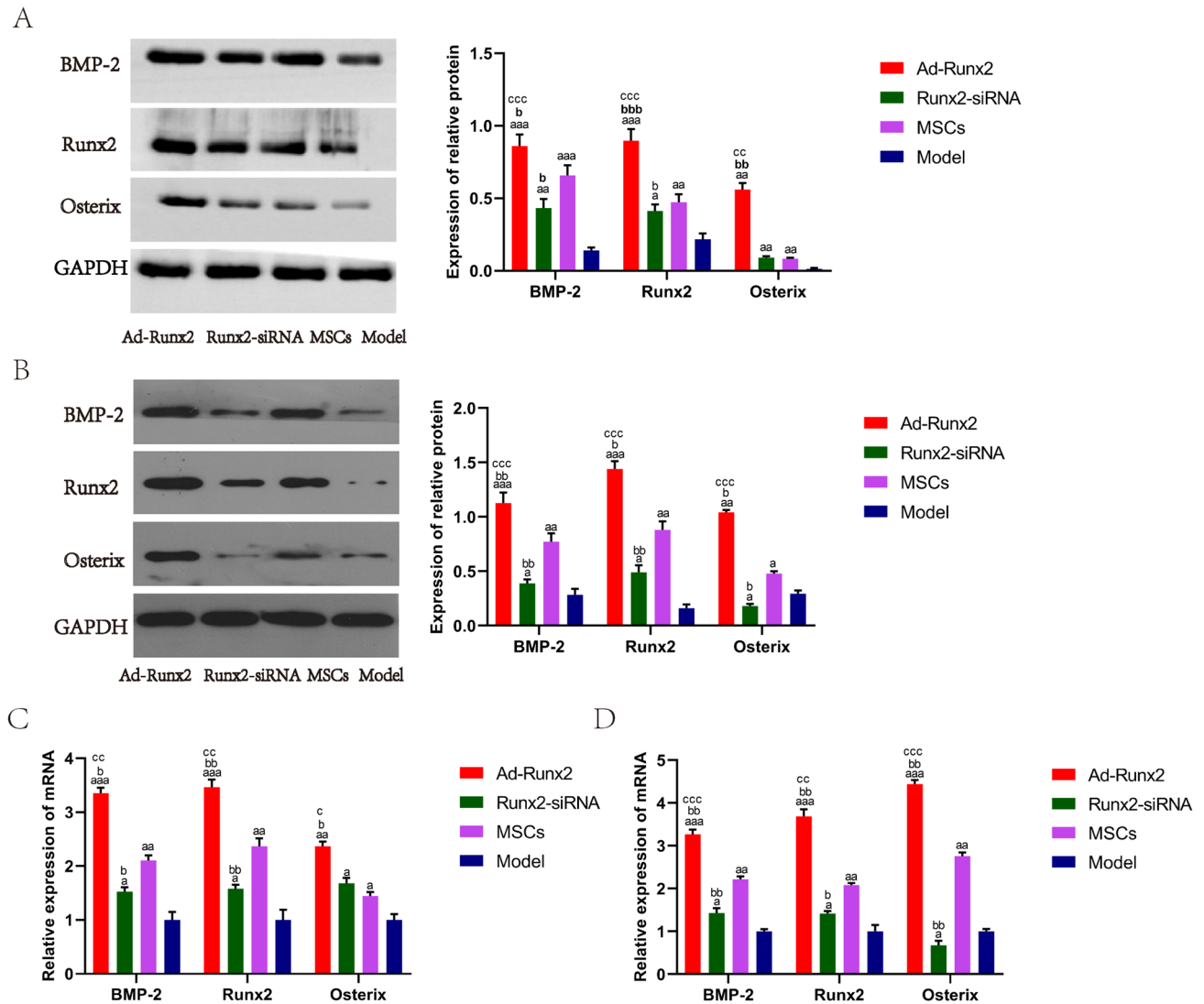


**Fig. 4** Up-regulated Runx2 accelerates osteonecrosis repair at 3 weeks and 6 weeks. **A** and **B** The BMP-2, Runx2 and Osterix determined by Western blot; **C** and **D** The BMP-2, Runx2 and Osterix determined by qPCR; <sup>a</sup>*P* < 0.05, <sup>aa</sup>*P* < 0.01 and <sup>aaa</sup>*P* < 0.001 com-

pared with the Model group; <sup>b</sup>*P* < 0.05, <sup>bb</sup>*P* < 0.01, <sup>bbb</sup>*P* < 0.001 compared with the MSCs group; <sup>c</sup>*P* < 0.05, <sup>cc</sup>*P* < 0.01, <sup>ccc</sup>*P* < 0.001 compared with the Runx2-siRNA group

inhibition of BMP-2 and Runx2 ( $P < 0.05$ ), and no difference of Osterix (Fig. 4A). The results of Western blot at 6 weeks revealed that compared with the Model group, the expression of BMP-2 and Runx2 were up-regulated significantly, and the expression of Osterix was down-regulated in the Runx2-siRNA group ( $P < 0.05$ ). Compared with the MSCs group, the Ad-Runx2 group presented a significantly augmented BMP-2, Runx2 and Osterix ( $P < 0.05$ ); However, the Runx2-siRNA group showed a significant inhibition of BMP-2, Runx2 and Osterix ( $P < 0.05$ ) (Fig. 4B). These results suggested that Runx2 overexpression can promote osteoblastic phenotype maintenance.

qPCR analysis at 3 weeks showed that compared with the Model group, the Ad-Runx2, Runx2-siRNA and MSCs groups exhibited significantly increased level of BMP-2, Runx2 and Osterix. Compared with the MSCs group, the expression of BMP-2, Runx2 and Osterix were further increased in the Ad-Runx2 group ( $P < 0.05$ ); However, the Runx2-siRNA group showed a significant inhibition of BMP-2 and Runx2 ( $P < 0.05$ ), and no difference of Osterix (Fig. 4C). qPCR analysis at 6 weeks showed compared with the Model group, the Runx2-siRNA group presented a significantly augmented BMP-2 and Runx2, and a significantly decreased Osterix (Fig. 4D). The results of qPCR analysis were basically consistent with Western blot.

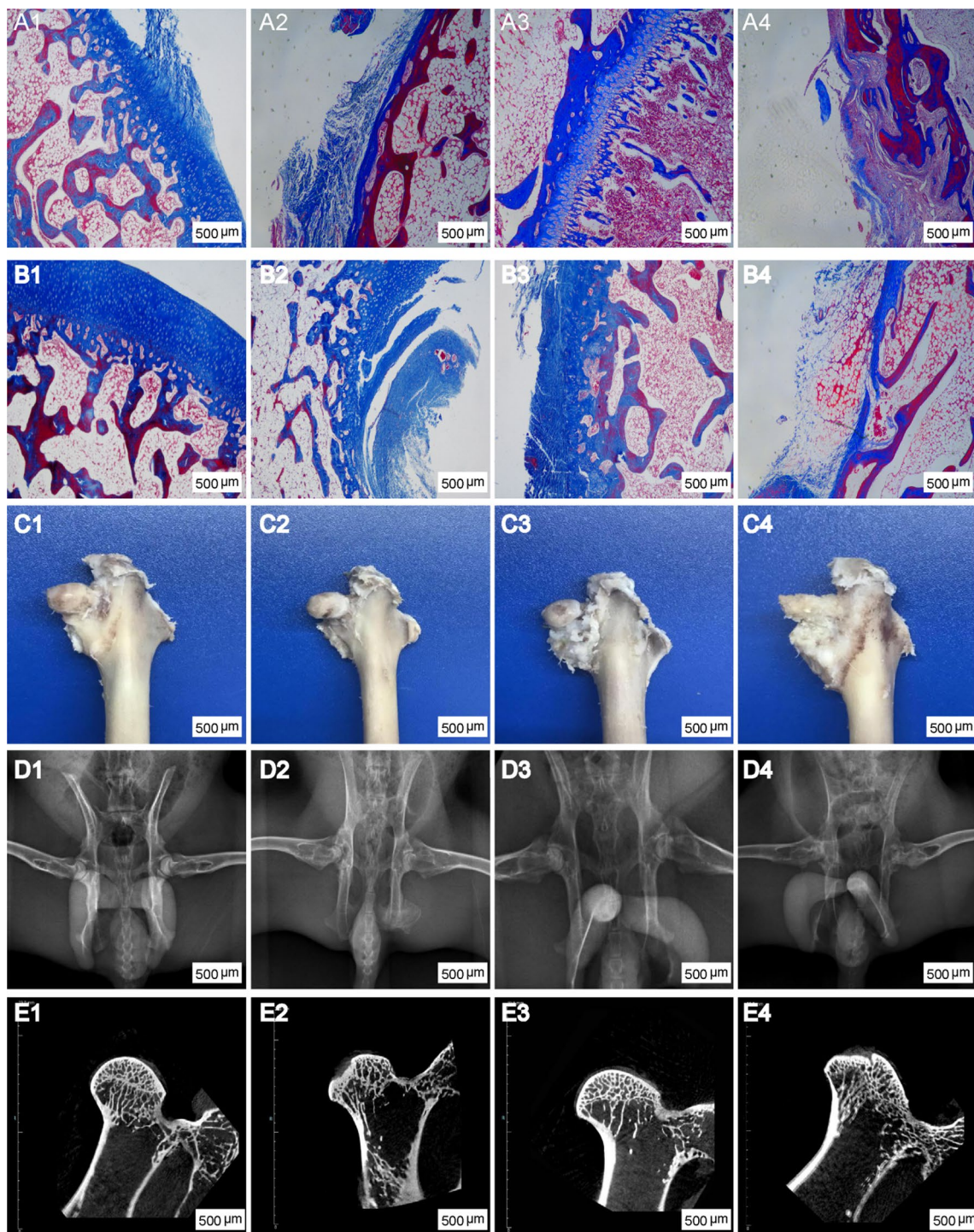


**Fig. 5** Overexpression of Runx2 promotes osteonecrosis repair. (A1–A4) and (B1–B4) Masson trichrome staining was used to evaluate the repair performance of necrotic femoral head at 3 and 6 weeks respectively; (C1–C4), (D1–D4) and (E1–E4) Gross morphology, X-ray and

Micro-CT were used to evaluate the repair performance of necrotic femoral head at 6 weeks; From left to right: Ad-Runx2 group, Runx2-siRNA group, MSCs group and Model group

### Masson trichrome staining, gross morphology and images observation findings of osteonecrosis repair

Masson trichrome staining was used to analysed histological changes of necrotic femoral head at 3 weeks and 6 weeks. The Model group resulted in obvious hollowing and inflammatory tissue at 3 weeks (Fig. 5A4). The osteonecrosis area

decreased after 6 weeks, and was covered by few fibrous tissue (Fig. 5B4). Compared with the Model group, the Runx2-siRNA group obtained small level repairment and was covered by few fibrous tissue and cartilage (Fig. 5A2 and B2). The Ad-Runx2 and MSCs groups obtained better repairment. Large amounts of fibrous tissue and cartilage covered the necrotic femoral head (Fig. 5A1 and A3). At 6 weeks, the regenerated tissue of Ad-Runx2 that contained rich cartilage and bone tissue basically completely covered the necrotic femoral head as indicated by Masson trichrome staining (Fig. 5B1).

The gross morphology, X-ray and CT images were used to evaluate the repair performance of necrotic femoral head at 6 weeks. The Model group had obvious bone defect and the morphology can barely be observed (Fig. 5C4). The Runx2-siRNA group showed collapsed femoral head, which has large bone defect and was covered by few cartilage (Fig. 5C2). More regular femoral head that was covered by cartilage appeared in the MSCs group (Fig. 5C3). In the Ad-Runx2 group, the necrotic femoral head was completely repaired and covered by hyaline cartilage, and the regenerated femoral head was smooth and regular (Fig. 5C1). Therefore, the results of gross morphology observation and Masson Trichrome Staining suggested that both MSCs group and Ad-Runx2 group have a obvious repairment, but Ad-Runx2 group produced better outcomes.

In the X-ray and CT images, the Model group showed the destruction of the femoral head, uneven density and disappeared joint space, the trabeculae in the subchondral bone was missing and disordered (Fig. 5D4 and E4); In the Runx2-siRNA group, the femoral head had irregular hemispherical shape, with uneven density and vesicular image, and the joint space was fuzzy, and the trabeculae was non-regular arrangement with massive fracture (Fig. 5D2 and E2); In the MSCs group, the femoral head was basically normal, with a small amount of high density shadow, and the joint space was slightly reduced, and the trabeculae was slightly disordered with a small amount of fracture (Fig. 5D3 and E3); The Ad-Runx2 group had normal morphology, uniform density and clear joint space, and the trabeculae was regular arrangement without fracture (Fig. 5D1 and E1); These results were basically consistent with the molecular experiments in vivo and in vitro.

## Discussion

Bone is a highly vascularized tissue, its blood supply accounts for about 10% of cardiac output. The oxygen concentration of the bone marrow is about 1~7% [27]. As we all know, the hypoxic microenvironment is often caused by injury or necrosis of bone and its surrounding soft tissue [28, 29]. There is different sensitiveness in the hypoxia

microenvironment among osteocytes, osteoclasts and osteoblasts, which means different survival times from 12 to 48 h. The accumulation of metabolites in the osteonecrosis area can aggravate the occurrence of apoptosis and death, and limit the self-repair ability of necrotic bone [30, 31]. As an important source of cell transplantation, MSCs can maintain activity and osteogenic differentiation ability in the hypoxic environment [32–34]. When MSCs are cultured under hypoxia, its proliferative capacity, alkaline phosphatase (ALP) activity, calcified nodule formation, neovascularization, vascularized bone regeneration and production of type I and type III collagen can be significantly induced [35–38]. The evidence provides theoretical support for the survival and differentiation ability of transplanted MSCs.

Osteogenic differentiation is the premise for treating ONFH. To date, many studies have shown that various transcription factors can affect the differentiation of MSCs toward osteoblasts, such as Runx2, osterix, and  $\beta$ -catenin. The Runx2 transcription factor has been proved that it is an essential inducer for bone formation and the osteogenic differentiation of MSCs [39–43]. Gao and his colleagues have demonstrated that Homeobox protein Hox-B7 (HOXB7) can enhance the osteogenic differentiation of MSCs by up-regulating Runx2 [44]. On the contrary, lack or mutation of Runx2 can lead to diseases. Cleidocranial dysplasia (CCD) will happen after mutations of Runx2, and bone formation will be severely impaired after lacking or inhibiting of Runx2 [45–48]. This research has proved that MSCs overexpressing Runx2 can improve osteogenic genes expression and maintain osteoblastic phenotype, and inhibition of Runx2 would lead to converse results.

Recently, some researchers have promoted Runx2 expression to improve bone formation in vivo. Zhao and his colleagues transfected MSCs with Runx2 by adenoviral vectors and implanted MSCs into mice. The data showed MSCs overexpressing Runx2 formed substantially more bone than cells transfected with control virus [49]. Byers and coworkers proposed a new method to improve bone formation through making tissue-engineered constructs using that consists of three dimensional polymeric scaffolds and MSCs overexpressing Runx2. Constructs were subsequently implanted into calvaria defects in rats, and micro-CT and histomorphometry were used to analyze bone healing. The data showed that Runx2-modified constructs contained twice as much bone as control constructs [50, 51]. In this study, we injected simple MSCs or MSCs that had been transfected with Ad-Runx2 or Runx2-siRNA into ONFH rabbit models, the results showed unsatisfactory results in the Runx2-siRNA group, the femoral head had irregular hemispherical shape, with uneven density and vesicular image, and the joint space was fuzzy, and the trabeculae was non-regular arrangement with massive fracture. The MSCs group achieved a certain repair effect, the femoral



head was basically normal, with a small amount of high density shadow, and the joint space was slightly reduced, and the trabeculae was slightly disordered with a small amount of fracture. The Ad-Runx2 group had a better effect, the femoral head had normal morphology, uniform density and clear joint space, and the trabeculae was regular arrangement without fracture, which meant necrotic femoral head was basically completely repaired after 6 weeks. This is the first study to induce MSCs directly by overexpressing Runx2 to treat ONFH.

## Conclusions

Our study showed that overexpression of Runx2 can improve the osteogenic differentiation potential of MSCs, and the repair effect of MSCs for treating ONFH. However, this study has some limitations. Firstly, Some experiments to verify changes of MSCs overexpressing Runx2 have not been completed, such as proliferation and migration. Secondly, more rabbits and detection time may be needed to provide more obvious comparisons.

**Author contributions** All authors contributed to the study conception and design. Material preparation, data collection and analysis were performed by [HJX], [XZL], [LY], [YN], [LLX] and [DMS]. The first draft of the manuscript was written by [HJX], [XZL] and [LY], and was proofread by [WL], [YY], and [ZHL]. All authors read and approved the final manuscript.

**Funding** This work was supported by the National Natural Science Foundation of China [Grant Numbers 81472103]; The Health Family Planning Research Fund of Wuhan City [Grant Number WX18M01 and WZ22Q13]; The Wuhan City Huanghe Talent Program, and the Wuhan Application Foundation Frontier Project [Grant Number 2019020701011471]. Knowledge Innovation Special Project of Wuhan Municipal Bureau of Science and Technology [Grant Number 2022020801010547].

## Declarations

**Competing interests** The authors have no relevant financial or non-financial interests to disclose.

**Ethical approval** All animal experiments were approved by the Ethics Committee of Wuhan Third Hospital, Tongren Hospital of Wuhan University, and followed the Guide for the Care and Use of Laboratory Animals.

**Open Access** This article is licensed under a Creative Commons Attribution 4.0 International License, which permits use, sharing, adaptation, distribution and reproduction in any medium or format, as long as you give appropriate credit to the original author(s) and the source, provide a link to the Creative Commons licence, and indicate if changes were made. The images or other third party material in this article are included in the article's Creative Commons licence, unless indicated otherwise in a credit line to the material. If material is not included in the article's Creative Commons licence and your intended use is not

permitted by statutory regulation or exceeds the permitted use, you will need to obtain permission directly from the copyright holder. To view a copy of this licence, visit <http://creativecommons.org/licenses/by/4.0/>.

## References

- Pouya F, Kerachian MA (2015) Avascular necrosis of the femoral head: are any genes involved? *Arch Bone Jt Surg* 3(3):149–155 PMID: 26213697
- Assouline-Dayan Y, Chang C, Greenspan A, Shoenfeld Y, Gershwin ME (2002) Pathogenesis and natural history of osteonecrosis. *Semin Arthritis Rheum* 32(2):94–124. <https://doi.org/10.1053/sarh.2002.33724b>
- Xu Y, Jiang Y, Xia C, Wang Y, Zhao Z, Li T (2020) Stem cell therapy for osteonecrosis of femoral head: Opportunities and challenges. *Regen Ther* 15:295–304. <https://doi.org/10.1016/j.reth.2020.11.003>
- Chen CY, Rao SS, Yue T, Tan YJ, Yin H, Chen LJ, Luo MJ, Wang Z, Wang YY, Hong CG, Qian YX, He ZH, Liu JH, Yang F, Huang FY, Tang SY, Xie H (2022) Glucocorticoid-induced loss of beneficial gut bacterial extracellular vesicles is associated with the pathogenesis of osteonecrosis. *Sci Adv* 8(15):eabg8335. <https://doi.org/10.1126/sciadv.abg8335>
- Houdek MT, Wyles CC, Martin JR, Sierra RJ (2014) Stem cell treatment for avascular necrosis of the femoral head: current perspectives. *Stem Cells Cloning* 7:65–70. <https://doi.org/10.2147/S1147.S36584>
- Liu G, Luo S, Lei Y, Jiao M, Cao R, Guan H, Tian R, Wang K, Yang P (2022) Osteogenesis-Related Long Noncoding RNA GAS5 as a novel biomarker for osteonecrosis of femoral head. *Front Cell Dev Biol* 10:857612. <https://doi.org/10.3389/fcell.2022.857612>
- Shen X, Luo J, Tang X, Chen B, Qin Y, Zhou Y, Xiao J (2022) Deep learning approach for diagnosing early osteonecrosis of the femoral head based on magnetic resonance imaging. *J Arthroplasty*. <https://doi.org/10.1016/j.arth.2022.10.003>
- Zhao P, Zhao S, Zhang J, Lai M, Sun L, Yan F (2022) Molecular Imaging of Steroid-Induced osteonecrosis of the femoral head through iRGD-Targeted Microbubbles. *Pharmaceutics* 14(9):1898. <https://doi.org/10.3390/pharmaceutics14091898>
- Pajarinen J, Lin T, Gibon E, Kohno Y, Maruyama M, Nathan K, Lu L, Yao Z, Goodman SB (2019) Mesenchymal stem cell-macrophage crosstalk and bone healing. *Biomaterials* 196:80–89. <https://doi.org/10.1016/j.biomaterials.2017.12.025>
- Shao F, Liu R, Tan X, Zhang Q, Ye L, Yan B, Zhuang Y, Xu J (2022) MSC Transplantation attenuates inflammation, prevents endothelial damage and enhances the angiogenic potency of endogenous MSCs in a model of pulmonary arterial hypertension. *J Inflamm Res* 15:2087–2101. <https://doi.org/10.2147/JIR.S355479>
- Hung SC, Pochampally RR, Chen SC, Hsu SC, Prockop DJ (2009) Angiogenic effects of human multipotent stromal cell conditioned medium activate the PI3K-Akt pathway in hypoxic endothelial cells to inhibit apoptosis, increase survival, and stimulate angiogenesis. *Stem Cells* 25(9):2363–2370. <https://doi.org/10.1634/stemcells.2006-0686>
- Mastrolia I, Giorgini A, Murgia A, Loschi P, Petrachi T, Rasini V, Pinelli M, Pinto V, Lolli F, Chiavelli C, Grisendi G, Baschieri MC, Santis G, Catani F, Dominici M, Veronesi E (2022) Autologous marrow mesenchymal stem cell driving bone regeneration in a rabbit model of femoral Head Osteonecrosis. *Pharmaceutics* 14(10):2127. <https://doi.org/10.3390/pharmaceutics14102127>

13. Li ZH, Liao W, Cui XL, Zhao Q, Liu M, Chen YH, Liu TS, Liu NL, Wang F, Yi Y, Shao NS (2011) Intravenous transplantation of allogeneic bone marrow mesenchymal stem cells and its directional migration to the necrotic femoral head. *Int J Med Sci* 8(1):74–83. <https://doi.org/10.7150/ijms.8.74>
14. Li Z, Liao W, Zhao Q, Liu M, Xia W, Yang Y, Shao N (2013) Angiogenesis and bone regeneration by allogeneic mesenchymal stem cell intravenous transplantation in rabbit model of avascular necrotic femoral head. *J Surg Res* 183(1):193–203. <https://doi.org/10.1016/j.jss.2012.11.031>
15. Takeuchi R, Katagiri W, Endo S, Kobayashi T (2019) Exosomes from conditioned media of bone marrow-derived mesenchymal stem cells promote bone regeneration by enhancing angiogenesis. *PLoS ONE* 14(11):e0225472. <https://doi.org/10.1371/journal.pone.0225472>
16. Jin YZ, Lee JH (2018) Mesenchymal stem cell therapy for bone regeneration. *Clin Orthop Surg* 10(3):271–278. <https://doi.org/10.4055/cios.2018.10.3.271>
17. Song F, Jiang D, Wang T, Wang Y, Lou Y, Zhang Y, Ma H, Kang Y (2017) Mechanical stress regulates osteogenesis and adipogenesis of rat mesenchymal stem cells through PI3K/Akt/GSK-3 $\beta$ / $\beta$ -Catenin signaling pathway. *Biomed Res Int* 2017:6027402. <https://doi.org/10.1155/2017/6027402>
18. Heydari Asl S, Hosseinpour H, Parivar K, Hayati Roodbari N, Hanaee-Ahvaz H (2018) Physical stimulation and scaffold composition efficiently support osteogenic differentiation of mesenchymal stem cells. *Tissue Cell* 50:1–7. <https://doi.org/10.1016/j.tice.201711.001>
19. Liu A, Lin D, Zhao H, Chen L, Cai B, Lin K, Shen SG (2021) Optimized BMSC-derived osteoinductive exosomes immobilized in hierarchical scaffold via lyophilization for bone repair through Bmpr2/Acvr2b competitive receptor-activated smad pathway. *Biomaterials* 272:120718. <https://doi.org/10.1016/j.biomaterials.2021.120718>
20. Liang Z, Luo Y, Lv Y (2020) Mesenchymal stem cell-derived microvesicles mediate BMP2 gene delivery and enhance bone regeneration. *J Mater Chem* 8(30):6378–6389. <https://doi.org/10.1039/d0tb00422g>
21. Chen J, Liu Z, Zhang H, Yang Y, Zeng H, Zhong R, Lai S, Liao H (2022) YBX1 promotes MSC osteogenic differentiation by activating the PI3K/AKT pathway. *Curr Stem Cell Res Ther*. <https://doi.org/10.2174/1574888X17666220805143833>
22. Shanbhag S, Al-Sharabi N, Mohamed-Ahmed S, Gruber R, Kristoffersen EK, Mustafa K (2022) Brief communication: Effects of conditioned media from human platelet lysate cultured MSC on osteogenic cell differentiation in vitro. *Front Bioeng Biotechnol* 10:969275. <https://doi.org/10.3389/fbioe.2022.969275>
23. Dalle Carbonare L, Bertacco J, Marchetto G, Cheri S, Deiana M, Minoia A, Tiso N, Mottes M, Valenti MT (2021) Methylsulfonylmethane enhances MSC chondrogenic commitment and promotes pre-osteoblasts formation. *Stem Cell Res Ther* 12(1):326. <https://doi.org/10.1186/s13287-021-02396-5>
24. Pokrovskaya LA, Nadezhdin SV, Zubareva EV, Burda YE, Gnezdyukova ES (2020) Expression of RUNX2 and osterix in rat mesenchymal stem cells during culturing in osteogenic-conditioned medium. *Bull Exp Biol Med* 169(4):571–575. <https://doi.org/10.1007/s10517-020-04931-5>
25. Kronenberg HM (2003) Developmental regulation of the growth plate. *Nature* 423(6937):332–336. <https://doi.org/10.1038/nature01657>
26. Li ZH, Liao W, Zhao Q, Huan T, Feng P, Wei X, Yi Y, Shao NS (2014) Effect of Cbfa1 on osteogenic differentiation of mesenchymal stem cells under hypoxia condition. *Int J Clin Exp Med* 7(3):540–548
27. Guitart AV, Debeissat C, Hermitte F, Villacreces A, Ivanovic Z, Boeuf H, Praloran V (2011) Very low oxygen concentration (0.1%) reveals two FDCP-Mix cell subpopulations that differ by their cell cycling, differentiation and p27KIP1 expression. *Cell Death Differ* 18(1):174–182. <https://doi.org/10.1038/cdd.2010.85>
28. Salim A, Nacamuli RP, Morgan EF, Giaccia AJ, Longaker MT (2004) Transient changes in oxygen tension inhibit osteogenic differentiation and Runx2 expression in osteoblasts. *J Biol Chem* 279(38):40007–40016. <https://doi.org/10.1074/jbc.M403715200>
29. Sun H, Xu J, Wang Y, Shen S, Xu X, Zhang L, Jiang Q (2023) Bone microenvironment regulative hydrogels with ROS scavenging and prolonged oxygen-generating for enhancing bone repair. *Bioact Mater* 24:477–496. <https://doi.org/10.1016/j.bioactmat.2022.12.021>
30. Kerachian MA, Harvey EJ, Cournoyer D, Chow TY, Séguin C (2006) Avascular necrosis of the femoral head: vascular hypotheses. *Endothelium* 13(4):237–244. <https://doi.org/10.1080/10623320600904211>
31. Weinstein RS, Nicholas RW, Manolagas SC (2000) Apoptosis of osteocytes in glucocorticoid-induced osteonecrosis of the hip. *J Clin Endocrinol Metab* 85(8):2907–2912. <https://doi.org/10.1210/jcem.85.8.6714>
32. Müller J, Benz K, Ahlers M, Gaissmaier C, Mollenhauer J (2011) Hypoxic conditions during expansion culture prime human mesenchymal stromal precursor cells for chondrogenic differentiation in three-dimensional cultures. *Cell Transpl* 20(10):1589–1602. <https://doi.org/10.3727/096368910X564094>
33. Markway BD, Tan GK, Brooke G, Hudson JE, Cooper-White JJ, Doran MR (2010) Enhanced chondrogenic differentiation of human bone marrow-derived mesenchymal stem cells in low oxygen environment micropellet cultures. *Cell Transpl* 19(1):29–42. <https://doi.org/10.3727/096368909X478560>
34. Cui Y, Li Z, Guo Y, Qi X, Yang Y, Jia X, Li R, Shi J, Gao W, Ren Z, Liu G, Ye Q, Zhang Z, Fu D (2022) Bioinspired Nanovesicles convert the skeletal Endothelium-Associated Secretory phenotype to treat osteoporosis. *ACS Nano* 16(7):11076–11091. <https://doi.org/10.1021/acsnano.2c03781>
35. Huang J, Deng F, Wang L, Xiang XR, Zhou WW, Hu N, Xu L (2011) Hypoxia induces osteogenesis-related activities and expression of core binding factor  $\alpha$ 1 in mesenchymal stem cells. *Tohoku J Exp Med* 224(1):7–12. <https://doi.org/10.1620/tjem.224.7>
36. Gu Q, Gu Y, Shi Q, Yang H (2016) Hypoxia promotes Osteogenesis of Human placental-derived mesenchymal stem cells. *Tohoku J Exp Med* 239(4):287–296. <https://doi.org/10.1620/tjem.239.287>
37. Hung SP, Ho JH, Shih YR, Lo T, Lee OK (2012) Hypoxia promotes proliferation and osteogenic differentiation potentials of human mesenchymal stem cells. *J Orthop Res* 30(2):260–266. <https://doi.org/10.1002/jor.21517>
38. Zhuang Y, Cheng M, Li M, Cui J, Huang J, Zhang C, Si J, Lin K, Yu H (2022) Small extracellular vesicles derived from hypoxic mesenchymal stem cells promote vascularized bone regeneration through the miR-210-3p/EFNA3/PI3K pathway. *Acta Biomater* 150:413–426. <https://doi.org/10.1016/j.actbio.2022.07.015>
39. Komori T (2006) Regulation of osteoblast differentiation by transcription factors. *J Cell Biochem* 99(5):1233–1239. <https://doi.org/10.1002/jcb.20958>
40. Varela N, Aranguiz A, Lizama C, Sepulveda H, Antonelli M, Thaler R, Moreno RD, Montecino M, Stein GS, van Wijnen AJ, Galindo M (2016) Mitotic inheritance of mRNA facilitates translational activation of the osteogenic-lineage commitment factor Runx2 in progeny of Osteoblastic cells. *J Cell Physiol* 231(5):1001–1014. <https://doi.org/10.1002/jcp.25188>
41. Almalki SG, Agrawal DK (2016) Key transcription factors in the differentiation of mesenchymal stem cells. *Differentiation* 92(1–2):41–51. <https://doi.org/10.1016/j.diff.2016.02.005>

42. Fregnani A, Saggin L, Giancesi K, Quotti Tubi L, Carraro M, Barilà G, Scapinello G, Bonetto G, Pesavento M, Berno T, Branca A, Gurrieri C, Zambello R, Semenzato G, Trentin L, Manni S, Piazza F (2022) CK1 $\alpha$ /RUNX2 Axis in the bone marrow micro-environment: a novel therapeutic target in multiple myeloma. *Cancers (Basel)* 14(17):4173. <https://doi.org/10.3390/cancers14174173>
43. Kim P, Park J, Lee DJ, Mizuno S, Shinohara M, Hong CP, Jeong Y, Yun R, Park H, Park S, Yang KM, Lee MJ, Jang SP, Kim HY, Lee SJ, Song SU, Park KS, Tanaka M, Ohshima H, Cho JW, Sugiyama F, Takahashi S, Jung HS, Kim SJ (2022) Mast4 determines the cell fate of MSCs for bone and cartilage development. *Nat Commun* 13(1):3960. <https://doi.org/10.1038/s41467-022-31697-3>
44. Gao RT, Zhan LP, Meng C, Zhang N, Chang SM, Yao R, Li C (2015) Homeobox B7 promotes the osteogenic differentiation potential of mesenchymal stem cells by activating RUNX2 and transcript of BSP. *Int J Clin Exp Med* 8(7):10459–70
45. Lee B, Thirunavukkarasu K, Zhou L, Pastore L, Baldini A, Hecht J, Geoffroy V, Ducy P, Karsenty G (1997) Missense mutations abolishing DNA binding of the osteoblast-specific transcription factor OSF2/CBFA1 in cleidocranial dysplasia. *Nat Genet* 16(3):307–310. <https://doi.org/10.1038/ng0797-307>
46. Otto F, Thornell AP, Crompton T, Denzel A, Gilmour KC, Rosewell IR, Stamp GW, Beddington RS, Mundlos S, Olsen BR, Selby PB, Owen MJ (1997) Cbfa1, a candidate gene for cleidocranial dysplasia syndrome, is essential for osteoblast differentiation and bone development. *Cell* 89(5):765–771. [https://doi.org/10.1016/s0092-8674\(00\)80259-7](https://doi.org/10.1016/s0092-8674(00)80259-7)
47. Chan WCW, Tan Z, To MKT, Chan D (2021) Regulation and role of transcription factors in Osteogenesis. *Int J Mol Sci* 22(11):5445. <https://doi.org/10.3390/ijms22115445>
48. Gayatri MB, Gajula NN, Chava S, Reddy ABM (2022) High glutamine suppresses osteogenesis through mTORC1-mediated inhibition of the mTORC2/AKT-473/RUNX2 axis. *Cell Death Discov* 8(1):277. <https://doi.org/10.1038/s41420-022-01077-3>
49. Zhao Z, Zhao M, Xiao G, Franceschi RT (2005) Gene transfer of the Runx2 transcription factor enhances osteogenic activity of bone marrow stromal cells in vitro and in vivo. *Mol Ther* 12(2):247–253. <https://doi.org/10.1016/j.ymthe.2005.03.009>
50. Byers BA, Guldberg RE, García AJ (2004) Synergy between genetic and tissue engineering: Runx2 overexpression and in vitro construct development enhance in vivo mineralization. *Tissue Eng* 10(11–12):1757–1766. <https://doi.org/10.1089/ten.2004.10.1757>
51. [51]Byers BA, Guldberg RE, Hutmacher DW, García AJ (2006) Effects of Runx2 genetic engineering and in vitro maturation of tissue-engineered constructs on the repair of critical size bone defects. *J Biomed Mater Res A* 76(3): 646-55. <https://doi.org/10.1002/jbm.a.30549>

**Publisher's Note** Springer Nature remains neutral with regard to jurisdictional claims in published maps and institutional affiliations.